Proc. Natl. Acad. Sci. USA
Vol. 81, pp. 3685–3689, June 1984
Biochemistry

Titin is an extraordinarily long, flexible, and slender myofibrillar protein

(striated muscle/cytoskeletal lattice/sarcomere/elastic filament)

KUAN WANG*†‡, RUBEN RAMIREZ-MITCHELL‡, AND DAWN PALTER†

*Clayton Foundation Biochemical Institute, †Department of Chemistry, and ‡Cell Research Institute, University of Texas, Austin, TX 78712

Communicated by Lester J. Reed, March 12, 1984

ABSTRACT **"Titin" is a term used to describe a pair of closely related megadalton polypeptides that together are the third most abundant myofibrillar protein in a wide range of striated muscles. It has been proposed that titin and another giant protein, nebulin, are the major components of an elastic cytoskeletal lattice within the sarcomere. We have now purified the leading band, titin-2 (T_2), of the titin doublet in native forms by extraction with Guba–Straub solution followed by chromatography. Electron microscopy of low-angle-shadowed and negatively stained specimens revealed that T_2 chains self-assembled into extremely long (from 0.1 μm to over 1.0 μm), flexible, and extensible slender strands (4–5 nm in diameter) with axial periodicity. Furthermore, these strands tended to associate to form filamentous bundles and meshworks. Thus, titin appears to be ideally suited as a component of an elastic lattice that serves as an organizing scaffold or template for thick and thin filaments.**

"Titin" is a term used to describe a pair of megadalton polypeptide chains that together are the third most abundant protein (8–12% of myofibrillar mass) in the sarcomeres of a wide range of skeletal and cardiac muscles (1, 2). The members of the titin doublet, designated as T_1 ($M_r \approx 1.4 \times 10^6$) and T_2 ($M_r \approx 1.2 \times 10^6$), have closely similar chemical composition and antigenic properties and appear to be a precursor–product pair (1–4). Although the functional role of titin remains to be determined, our localization studies have led us to propose that titin and another giant protein, nebulin ($M_r \approx 0.6 \times 10^6$) (3), are the major components of an elastic cytoskeletal lattice that coexists with thick and thin filaments within the sarcomere (5–7). A hypothetical three-filament sarcomere model incorporating this cytoskeletal lattice has been described recently (6, 7). It is thought that this lattice may serve as a dynamic scaffold or organizing template with which discontinuous thick and thin filaments may interact, thereby imparting structural or perhaps functional continuity to the sarcomere (see ref. 7 for further discussions). To evaluate the validity of this proposal, it is critical to understand the basic morphological features and assembly properties of major components of this lattice. Unfortunately, intact titin (T_1) and nebulin are difficult to extract from myofibrils with benign solvents, and successful purification of both proteins has so far required the continuous presence of strong denaturants such as sodium dodecyl sulfate, urea, or guanidinium chloride (1–3).

We have now succeeded in purifying T_2, the leading band of the titin doublet, in the complete absence of denaturants. This has allowed us to study its morphology and interaction with other myofibrillar proteins. We report here the purification procedure and the findings that titin molecules assemble into extremely long, flexible, slender, and extensible filamentous strands that are ideally suited as cytoskeletal filaments. Preliminary reports have appeared in meeting abstracts (4, 8, 9).

The publication costs of this article were defrayed in part by page charge payment. This article must therefore be hereby marked "*advertisement*" in accordance with 18 U.S.C. §1734 solely to indicate this fact.

EXPERIMENTAL PROCEDURES

Purification of Native T_2 from Rabbit Skeletal Muscle. Fresh rabbit back muscle (50 g) was blended with 250 ml of Guba–Straub solution (0.3 M KCl/0.15 M KP_i, pH 6.7), extracted for 60 min, and centrifuged at 8000 rpm for 30 min in a Sorvall GSA rotor. Powdered ammonium sulfate was added with stirring to the supernatant (24.1 g/100 ml) over 20 min to precipitate myosin, C protein, and titin. The suspension was centrifuged at 8000 rpm for 15 min and the precipitate was redissolved in ≈25 ml of 0.15 M KP_i/10 mM EDTA, pH 7.5. After dialysis overnight against the same buffer, the sample was applied to a 2.5 × 30 cm DEAE-Sephadex (A50, Pharmacia) column equilibrated with the same buffer. The flow-through fractions were pooled, dialyzed against 0.01 M KP_i/0.1 M NaCl/0.1 mM dithiothreitol, pH 7.8, overnight and applied to a 2 × 20 cm hydroxyapatite (Bio-Rad HTP) column. A two-step elution was used, including a step gradient of 1 column volume (≈60 ml) of 0.15 KP_i/0.1 M NaCl/0.1 mM dithiothreitol, pH 7.8, to elute C protein and a linear gradient of 3 column volumes each of 0.15 M KP_i/0.1 M NaCl/0.1 mM dithiothreitol at pH 7.8, and 0.5 M KP_i/0.1 M NaCl/0.1 mM dithiothreitol, pH 7.8, to resolve remaining C protein and T_2 (which was eluted as a broad peak between 0.25 and 0.30 M KP_i). The peak and trailing fractions of the T_2 peak were free of C protein (>95% pure, yield ≈20 mg/50 g of muscle). For electron microscopy, T_2 was purified further on a Sephacryl S-1000 (Pharmacia) gel filtration column to remove some aggregated material. Fractions were concentrated to 3 mg/ml (by dry dialysis against polyethylene glycol), dialyzed against 1.0 M KCl/10 mM Tris·HCl/5 mM EDTA/0.1 mM dithiothreitol, pH 8.0, and applied to a 2 × 96 cm Sephacryl S-1000 column in the same buffer. T_2 was eluted in two peaks, one at half-column volume and another at two-thirds column volume, both showing only one T_2 band on sodium dodecyl sulfate gels. The second peak, containing presumably more dispersed T_2, was chosen for detailed morphology studies. Electropherograms of samples from the various stages of purification are shown in Fig. 1.

Electron Microscopy. For low-angle rotary shadowing, freshly gel filtered T_2 (0.2 mg/ml) was dialyzed overnight at 4°C against a large volume of 0.5 M KCl (or 0.5 M ammonium formate)/0.1 mM dithiothreitol, pH 8.0, and diluted to 1–10 μg/ml with the same buffer immediately before spraying onto a perpendicular (90°) or tilted (135°) mica surface (10). A simple spraying technique requiring only 20–50 μl of sample was developed. A plastic pipet tip was loaded with the protein solution and was taped onto the sloped nozzle (Fullam no. 51690) of a Freon duster such that the pipet opening was directly in the spray path. A fine mist of protein droplets was

Abbreviation: Da, dalton(s).

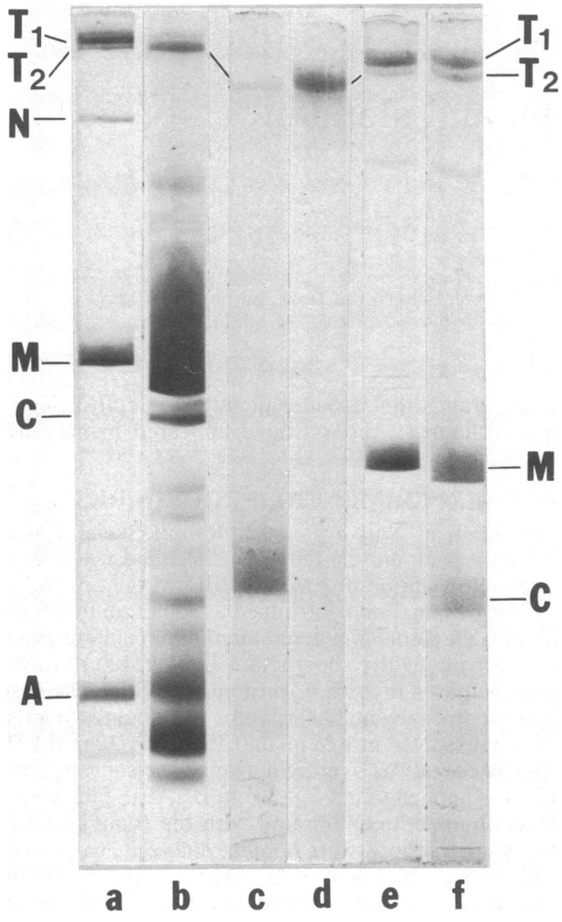

FIG. 1. Gel electrophoresis in the presence of sodium dodecyl sulfate and reducing agent was performed on high-porosity 3.2% polyacrylamide tube gels as described (2). N, nebulin; M, myosin heavy chain; C, C protein; A, actin. Lane a, rabbit myofibril (70 μg); lane b, high-salt extract (200 μg); lane c, flow-through fractions of DEAE-Sephadex column (crude C protein) (20 μg); lane d, T_2 peak of hydroxyapatite column (20 μg); lanes e and f, prolonged electrophoresis of rabbit myofibrils (50 μg) (e) and a mixture of myofibrils (20 μg) and DEAE-Sephadex flow-through (10 μg) (f).

then sprayed onto mica flakes at a distance of about 10 cm. The sample was dried at room temperature [1×10^{-5} torr in a Balzers (Liechtenstein) BAF400D] and rotary shadowed at low angle (5–10°) with platinum/carbon. The replica was floated on water, picked up on 400 mesh copper grids, and observed in a JEOL 100CX microscope at 80 kV. All micrographs of shadowed specimens were printed in reverse contrast.

RESULTS

Purification of Rabbit Skeletal Muscle T_2. In pilot experiments, we observed that most of the high-salt solutions commonly used to extract thick filament proteins also extracted a portion of T_2. The preferential extraction of T_2 relative to T_1 by these A band solvents is illustrated in Fig. 1, lane b, where a Guba–Straub extract exhibited a very high T_2-to-T_1 ratio. In contrast, intact rabbit myofibril had a low T_2-to-T_1 ratio of 0.2 to 0.3 (Fig. 1, lane a). Following these clues, we have successfully developed several procedures to purify T_2. The procedures described in the *Experimental Procedures* were derived from the C protein protocols (11, 12). Changes and additional steps were introduced to enhance extraction of T_2 and to achieve better resolution of C protein and T_2 on the hydroxyapatite column (Fig. 1, lane d). This procedure, despite its modest yield (≈20 mg of T_2 from 50 g of muscle), has the advantage that myosin and C protein were purified simultaneously from the same muscle extract. We noted that a very small amount of T_1 was frequently extracted, but it was invariably lost at the end; presumably, it had degraded or remained tightly bound to the DEAE-Sephadex or hydroxyapatite columns. Freshly prepared T_2 consisted of only one band on sodium dodecyl sulfate gels and was free of myosin and C protein (>95% purity) (Fig. 1, lanes d, e, and f). However, storage at 4°C frequently caused the preparation to appear as a doublet or multiple bands that had very similar mobility and staining intensity to those of the T_1 and T_2 doublet in intact myofibril. However, upon closer examination with coelectrophoresis techniques, they were found to represent T_2 and its degradation products (data not shown).

Molecular Morphology of Native Titin (T_2). For electron microscopy, native T_2 was purified further on a Sephacryl S-1000 gel filtration column under ionic conditions that favored the dissociated state of the aggregation-prone protein (i.e., high salt and alkaline pH values; unpublished observations). The second T_2 peak, presumably being more dispersed material, was used for the present work. As shown in Fig. 2*a*, low-angle rotary-shadowed T_2 appeared predominantly as very long, flexible, filamentous strands with irregularly spaced sharp bends and kinks. The strand appeared flexible along all its length since there was no evidence of preferential bending at specific loci. The width appeared uniform along the length and was the same for all well-extended strands in a given specimen. However, at higher power, many strands had a beaded morphology (circles, Fig. 2*b*). It was also consistently observed that some of the strands had large globular nodules of various sizes (labeled as n in Fig. 2 *a* and *c*) attached either at the ends or along the length. Presumably, these nodules arose from coiling of the extremely flexible strands during sample preparation.

Because contour length of such convoluted molecules was difficult to measure with precision, we sought ways to extend more fully the titin strand. Some success was achieved in two (out of four) preparations in which protein solutions were sprayed onto a tilted (45°) mica surface. Many fields were found to contain groups of parallel, fully extended, nearly linear titin strands, presumably resulting from favorable flow conditions on tilted surfaces (Fig. 2 *c* and *d*). Many linearized strands possessed one or more sharp turns, to give rise to double-stranded or multiple-stranded regions (ds and ms in Fig. 2*c*). The width of each strand in the multistranded region was much thinner than that of the single-stranded region on the same strand, due to the blockage of shadowing by closely apposed strands. There was no evidence of a preferred length for the multistranded region, suggesting again a uniform flexibility along the strand. Nodules were more abundant in these tilt-sprayed preparations.

Width, Length, Axial Periodicity, and End-to-End Association of Titin Strands. The width of shadowed strands varied from 7 to 12 nm for several different preparations, depending on shadowing conditions. To estimate the width of naked strands, two approaches were used to correct for replica thickness. First, a small amount of rabbit myosin was added as an internal standard (circle in Fig. 2*d*). Assuming that the naked myosin tail, which measured 5 nm in this shadowed sample, is 2 nm wide, the width of a naked titin strand was about (7 to 9 nm) − 3 nm = 4 to 6 nm. A second approach required no internal standards and was performed according to Heuser (13) on molecules having closely apposed double-stranded regions (cf. Fig. 2*c*). The width of a single naked titin strand was 13 to 14 nm (edge-to-edge width of shadowed double strands) − 9 nm (width of shadowed single strand) = 4 to 5 nm, in fair agreement with the first estimate.

A histogram of contour length of well-extended, nodule- and gap-free strands in 0.5 M KCl buffer is shown in Fig. 2*i*. Titin strands were 0.1 μm to well over 1.0 μm, and the fre-

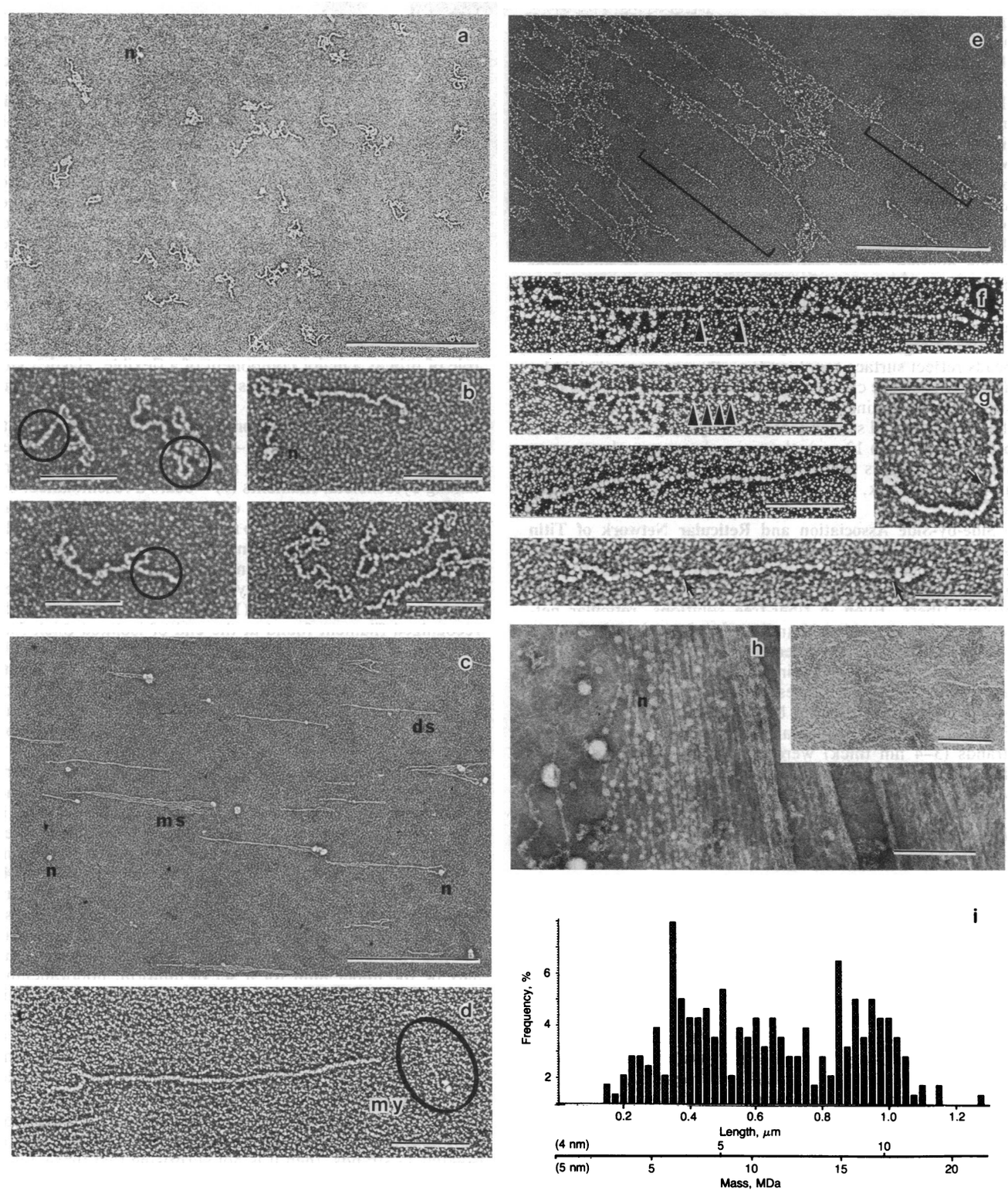

FIG. 2. Molecular morphology of native T_2. (*a–g*) Low-angle rotary shadowing. (*a*) Highly convoluted titin strands (0.5 M ammonium formate buffer) (bar = 1 μm). (*b*) Selected high-power views of *a*. Note the beaded string morphology (circles) and the nodules (n) (bar = 0.2 μm). (*c*) Linearized titin strands on tilt-sprayed mica (in 0.5 M KCl buffer). Note the double-stranded (ds) or multistranded (ms) regions and nodules (n) (bar = 1 μm). (*d*) Selected high-power view of *c*. Note the relative dimension of titin and myosin (my). The beaded string morphology is less conspicuous in this sample and titin strands appear uniform in width (bar = 0.2 μm). (*e*) Reticular network of titin strands (in 0.5 M KCl). Note the thinning of many strands (brackets) (bar = 1 μm). (*f* and *g*) Selected high-power view of *e*. Note the different thickness of these strands and the irregularly spaced beads (arrowheads) (bar = 0.2 μm). (*h*) Negatively stained titin network. The same T_2 solution (50 μg/ml in 0.5 M KCl buffer) used for rotary shadowing in *c* was stained with 2% unbuffered uranyl acetate. Note the filament bundles and nodules (n). *Inset* shows fine titin strands on the background (bar = 0.2 μm; *Inset*, bar = 50 nm). Note that *h* is at the same magnification as *b*, *d*, *f*, and *g*. (*i*) Histogram of number frequency vs. contour length. A total of 250 well-extended strands from a 0.5 M KCl sample were measured to 0.01 μm precision and plotted at 0.025-μm intervals. Mass was calculated for either 4 nm diameter or 5 nm diameter, assuming the strands are uniform cylinders with partial specific volume of 0.73 ml/g. MDa, megadaltons.

quency curve showed peaks near 0.11, 0.23, 0.37, 0.43, 0.65, and 0.96 μm. Such a heterodisperse distribution suggested that end-to-end association of titin strands had occurred to various degrees. This conclusion is supported by the fact that the majority of these strands were multimillion daltons in mass and therefore contained more than one T_2 polypeptide chain (up to 20–25; see calculated mass scales in Fig. 2*i*). Most interestingly, the multiple peaks in the diagram appeared to be integral multiples of 0.11–0.12 μm, which correspond in mass to about one T_2 chain (4-nm-diameter strand) or two T_2 chains (5-nm-diameter strands). If this is correct, then the end-to-end association must occur without appreciable overlap, since well-extended strands of all lengths have the same uniform width with no protrusions.

The presence of somewhat regular or perhaps periodic axial substructures was suggested by the beaded morphology (circles in Fig. 2*b*). It is not yet clear, however, whether the beads reflect surface topology (i.e., the presence of globular domains), surface chemistry (i.e., the presence of nucleation sites of metal grains), or both. We observed that, although the values of bead size and interbead spacing varied between preparations (7 to 12 nm), the two values were always very similar. Thus, it is probable that if the unshadowed strands are 4 to 5 nm thick, the periodicity might also be as small as 4 to 5 nm.

Side-by-Side Association and Reticular Network of Titin Strands. Titin strands are extremely prone to aggregation, especially at air/water interfaces. Gentle pipetting of titin solution invariably caused the appearance of visible stringy protein fibers. Even in fiber-free solutions, reticular networks of titin strands and bundles of various sizes frequently coexisted with the dispersed strands (rotary shadowed in Fig. 2 *e* and *f*, negatively stained in Fig. 2*h*). In addition, very large nodules of various sizes were seen decorating the fiber bundles, especially near the boundary of the network (n's in Fig. 2*h*). In negatively stained samples, very fine titin strands (3–4 nm thick) were observed in the background (Fig. 2*h*, *Inset*). The overall morphology of the fibrous network suggests that long titin strands must associate end-to-end as well as side-by-side to form long bundles of various sizes and to form networks. Strands with only one end attached to the network tended to coil up to form large nodules.

Extensibility and Discontinuity of Titin Strands. Many strands in the reticular network showed a gradual thinning in diameter and, in extreme cases, became invisible (i.e., thinner than the size of platinum grains—about 2 nm) (brackets in Fig. 2*e*). Interestingly, the beaded structure or small nodules in such strands became more irregularly and widely spaced (arrowheads in Fig. 2*f*; cf. Fig. 2*b*). Even in fields of dispersed titin strands, we occasionally found gaps or abrupt discontinuities along the strands (arrows in Fig. 2*g*). These images suggest that titin strands are fragile and are easily extensible along the strands when subjected to stress during sample preparation or drying. It is conceivable that titin polypeptides have either unfolded or slid within the strands or broken at certain loci.

DISCUSSION

The successful purification of native T_2 is a significant step toward a systematic study of the molecular properties of titin and the search for its interactions with other muscle proteins.[§]

Our electron miscroscopy data indicate that in solution T_2 chains tend to self-assemble to form extremely long (0.1 to over 1.0 μm), flexible, unbranched, extensible thin strands (4–5 nm diameter) with axial periodicity (as yet undefined, probably 4–5 nm). The general appearance of T_2 is thus strikingly similar to that of several well-studied long, flexible cytoskeletal structural proteins, such as fibronectin (e.g., ref. 14), filamin, or spectrin (e.g., ref. 15), except that the titin appears much more flexible. Such a similarity may reflect a basic molecular design of a class of adhesive molecules that function as an organizing scaffold or template for target molecules and cellular components. All of the molecules possess multiple binding domains that are linearly encoded on a very long, flexible strand. Additionally, the self-assembly properties of T_2 (end-to-end and side-by-side association), extensibility (elasticity?), and axial periodicity are all desirable and indeed essential attributes for the proposed role of titin as a major component of a flexible, elastic cytoskeletal lattice that serves as a scaffold for thick and thin filaments (see ref. 7).

It is significant that the morphology of both gap filaments (16) and end filaments (17)—two ultrastructural features that we previously proposed as manifestations of titin-containing cytoskeletal filaments (7)—bears a resemblance, especially in thickness, to that of T_2 strands in solution. Gap filaments, which span the gap regions between A bands and I bands in overly stretched, nonoverlapping sarcomeres (>3.7 μm), have a stretch-dependent thickness that varied from 3 to 6 nm, and they frequently exhibit a nodular or beaded appearance in thin sections (16). End filaments, a recently recognized filament found at the end of isolated thick filaments (17), have dimensions of 5 × 85 nm with occasionally a nodular end. The comparable diameter of these filaments and T_2 strands suggests the intriguing possibility that the titin-containing region of the cytoskeletal lattice *in situ* may have a similar (but not necessarily identical) organization and state of assembly as the isolated T_2 strands.

Additional clues about titin organization in the sarcomere can be obtained by a consideration of the mass content and sarcomeric distribution of titin. It can be estimated[¶] that, if titin filaments span the distance between a pair of N_2 lines across the A band (about 1.8 μm in a sarcomere of 2.5 μm; see ref. 7), the total mass of titin is equivalent to about two 4-nm × 1.8-μm cylindrical strands, or one 5-nm × 1.8-μm strand per thick filament. Since it is unlikely that there is less than one titin filament per thick filament (recall that there is one gap filament per thick filament), the 5-nm diameter thus may be the upper limit for a set of uniform, nonbranching titin filaments to assume *in situ*. Clearly, many more complicated arrangements are possible if titin filaments are allowed to branch or to fork. For example, an arrangement with two 4-nm strands within the A band that then coalesce into a single 5-nm strand at certain points outside the A band would equally satisfy the stated mass and length constraints.

If the titin region of the cytoskeletal lattice in the sarcomere indeed resembles the appearance and organization of isolated T_2 strands, then it is not surprising that these cytoskeletal filaments have been so elusive. In plastic sections of normal overlapping sarcomeres, the slender, stretchable fila-

[§]It should be noted that T_2 is a large fragment representing 85% of the mass of intact titin T_1. While it is conceivable that the missing 15% may impart additional structural features, it is reasonable to expect that the properties described here for T_2 will prevail for T_1 as well. We suspect that the missing portion (≈200 kDa) is somehow involved in anchoring T_1 to certain high-salt-resistant sarcomeric structures, thus rendering T_1 difficult to extract.

[¶]It is calculated by assuming the following range of values: mass ratio of titin (T_1 plus T_2) to myosin heavy chain = 0.25 to 0.30 (ref. 2); mass content of titin strands = 10×10^7 Da/μm (for 4 nm diameter) or 17×10^7 Da/μm for 5 nm diameter (Fig. 2*i*); length of titin strands in a 2.5-μm sarcomere = 1.8 μm (N_2 to N_2 across the A band, see ref. 7); mass content of myosin heavy chain per thick filament = 200,000 × 300 × 2 Da = 12.0×10^7 Da. Therefore, the range of ratios of the titin strand to thick filament is 0.25 [to 0.30]/($1.8 \times 10 \times 10^7$) divided by $1.0/(12 \times 10^7)$ = 1.7 to 2.0 (for 4-nm strands); or 0.25 [to 0.30]/($1.8 \times 17 \times 10^7$) divided by $1.0/(12 \times 10^7)$ = 1.0 to 1.2 (for 5-nm strands).

ments would be difficult to resolve and to contrast adequately against the background of thick and thin filaments and abundant cross-bridges. In preparations of isolated muscle components, titin may assume such a multitude of guises (thin strands of variable thickness, nodules of various sizes, fiber bundles, and reticular networks) that identification by morphological criteria alone may be equally difficult.[||] However, given the rapid advances in new morphological and immunocytological techniques, a basic understanding of the overall organization of these novel cytoskeletal filaments should be a realistic goal, with the morphology of "synthetic" titin strands as a guide.

While this paper was being reviewed, Kimura and Maruyama (20) reported a purification procedure for native chicken connectin. We also learned that Trinick *et al.* (21) have purified and characterized native rabbit psoas titin. Their morphological data on titin are in substantial agreement with ours. It is not yet clear whether the proteins studied by these two groups are T_1, T_2, or other derivatives of titin.

[||]In a survey of published electron micrographs of isolated native thick filaments, we noticed examples of the presence of slender filaments that lay alongside and parallel to the thick filaments (e.g., plate IIa of ref. 18; figure 1 of ref. 19). These filaments appeared to be thinner than the thin filaments in the same field and could have been titin strands.

We thank John Wright for his assistance in histogram measurements. We thank Dr. J. Trinick for sending us a preprint of ref. 21. This work is supported in part by grants from the National Institutes of Health (AM20270) and the American Heart Association, Texas Affiliate.

1. Wang, K., McClure, J. & Tu, A. (1979) *Proc. Natl. Acad. Sci. USA* **76**, 3698–3702.
2. Wang, K. (1982) *Methods Enzymol.* **85**, 264–274.
3. Wang, K. & Williamson, C. L. (1980) *Proc. Natl. Acad. Sci. USA* **77**, 3254–3258.
4. Wang, K. & Ramirez-Mitchell, R. (1982) *Biophys. J.* **37**, 45 (abstr.).
5. Wang, K. & Ramirez-Mitchell, R. (1979) *J. Cell Biol.* **83**, 389 (abstr.).
6. Wang, K. (1982) in *Muscle Development, Molecular and Cellular Control*, eds. Pearson, M. L. & Epstein, H. F. (Cold Spring Harbor Laboratory, Cold Spring Harbor, NY), pp. 439–452.
7. Wang, K. (1984) in *Contractile Mechanisms in Muscle*, eds. Sugi, H. & Pollack, G. H. (Plenum, New York), pp. 285–306.
8. Wang, K. & Ramirez-Mitchell, R. (1982) *J. Cell Biol.* **95**, 372 (abstr.).
9. Wang, K. & Ramirez-Mitchell, R. (1983) *Biophys. J.* **41**, 96 (abstr.).
10. Tyler, J. M. & Branton, D. (1980) *J. Ultrastruct. Res.* **71**, 95–102.
11. Offer, G., Moos, C. & Starr, R. (1973) *J. Mol. Biol.* **74**, 654–676.
12. Starr, R. & Offer, G. (1982) *Methods Enzymol.* **85**, 130–138.
13. Heuser, J. E. (1983) *J. Mol. Biol.* **169**, 155–195.
14. Erickson, H. P., Carrell, N. & McDonagh, J. (1981) *J. Cell Biol.* **91**, 673–678.
15. Tyler, J. M., Anderson, J. M. & Branton, D. (1980) *J. Cell Biol.* **85**, 489–495.
16. Locker, R. H. & Leet, N. G. (1975) *J. Ultrastruct. Res.* **52**, 64–75.
17. Trinick, J. (1981) *J. Mol. Biol.* **151**, 309–314.
18. Huxley, H. E. (1963) *J. Mol. Biol.* **7**, 281–308.
19. Trinick, J. & Elliott, A. (1979) *J. Mol. Biol.* **131**, 133–136.
20. Kimura, S. & Maruyama, K. (1983) *J. Biochem. (Tokyo)* **94**, 2083–2085.
21. Trinick, J., Knight, P. & Whiting, A. (1984) *J. Mol. Biol.*, in press.